China Geology 8 (2025) 77−91

China Geology

Journal homepage: http://chinageology.cgs.cn
https://www.sciencedirect.com/journal/china-geology

Evaluating the hydrocarbon generation potential of the Paleocene–Eocene carbonaceous rocks in the Barmer and Bikaner-Nagaur Basins, western Rajasthan, India

Alok Kumar[a, b], Khairul Azlan Mustapha[a,*], Alok K. Singh[c], Mohammed Hail Hakimi[d], Ali Y. Kahal[e], Waqas Naseem[a, f], Hijaz Kamal Hasnan[a]

[a] *Department of Geology, Faculty of Science, Universiti Malaya, Kuala Lumpur* 50603, *Malaysia*
[b] *Department of Geology, Institute of Science, Banaras Hindu University, Varanasi* 221005, *India*
[c] *Department of Petroleum Engineering and GeoEngineering, Rajiv Gandhi Institute of Petroleum Technology, Jais* 229304, *India*
[d] *Institute of Geology and Petroleum Technologies, Kazan Federal University, Kazan* 420008, *Russia*
[e] *Geology and Geophysics Department, King Saud University, Riyadh* 11451, *Saudi Arabia*
[f] *Department of Geology, University of Poonch, Rawalakot* 12350, *Pakistan*

ARTICLE INFO

Article history:
Received 20 October 2023
Received in revised form 16 December 2023
Accepted 1 January 2024
Available online 11 September 2024

Keywords:
Carbonaceous shale
Petroliferous
Bikaner-Nagaur Basin
Barmer Basin
High hydrogen index
Hydrogen-rich kerogen
Western Rajasthan
Geochemistry
Petrology

ABSTRACT

The Bikaner-Nagaur and Barmer Basins (Rajasthan) are the most important petroliferous sedimentary basins in India. For over a decade, the exploration and extraction of hydrocarbons in these basins. Paleocene-Eocene age rocks bear organic-rich sediments in these basins, including lignite and carbonaceous shale deposits. The present research investigates the source rock properties, petroleum potential and thermal maturity of the carbonaceous shale partings from the lignite mines of Gurha (Bikaner-Nagaur Basin) and Kapurdi (Barmer Basin) using petrographical and geochemical tools. The carbonaceous shales have high organic matter (OM), with considerable total organic carbon (TOC) contents ranging from 13% to 39%. Furthermore, they contain hydrogen-rich kerogen, including types II and II/III, as evidenced by the Rock-Eval and elemental analysis results. The existence of these kerogen types indicates the abundance of reactive (vitrinite and liptinite) macerals. However, the carbonaceous shales from the Bikaner–Nagaur Basin have oil generation potentials, with a high hydrogen index (up to 516 mg HC/g TOC) and a H/C ratio (up to 1.5) along with a significant presence of oil-prone liptinitic macerals. Apart from the geochemical and petrological results, the studied shales have low huminite reflectance (0.31%–0.48%), maximum temperature (S_2 peak; T_{max}) between 419°C and 429°C, and low production index values (PI: 0.01–0.03). These results indicate that these carbonaceous shales contain immature OM, and thereby, they cannot yet release commercial amount of oil. This immaturity level in the studied outcrop section is due to the shallow burial depth. Geochemical proxies further indicate the presence of both oil and gas-prone source rocks.

1. Introduction

Unconventional petroleum resources are attracting considerable interest globally because of the increasing energy demands (Mukherjee M and Misra S, 2018). There are 26 proliferous sedimentary basins in India containing conventional and unconventional petroleum resources (Directorate General of Hydrocarbons, India). The state of Rajasthan features the largest hydrocarbon-containing sedimentary basin. Based on the exploration activity and the occurrence of petroleum in Rajasthan, this basin is categorized under category-I (i.e., having a proven hydrocarbon reserve and already producing petroleum). Rajasthan, which is a component of the Indian Shield, has sedimentary sequence from the Archean to Recent eras. The state contains four basins, the Barmer, Bikaner-Nagaur, Jaisalmer, and Sanchore basins, which were developed by intracratonic sedimentation and are mostly located in the western part of Rajasthan (Fig. 1a). These basins feature a huge lignite reserve containing thick organic-rich carbonaceous shale partings, which can be exploited as source

First author: *E-mail address*: alok.gly@gmail.com (Alok Kumar).

* Corresponding author: *E-mail address*: azlan.geo@gmail.com (Khairul Azlan Mustapha).

Literary editor: Xi-jie Chen
doi:10.31035/cg20230121
2096-5192/© 2025 China Geology Editorial Office.

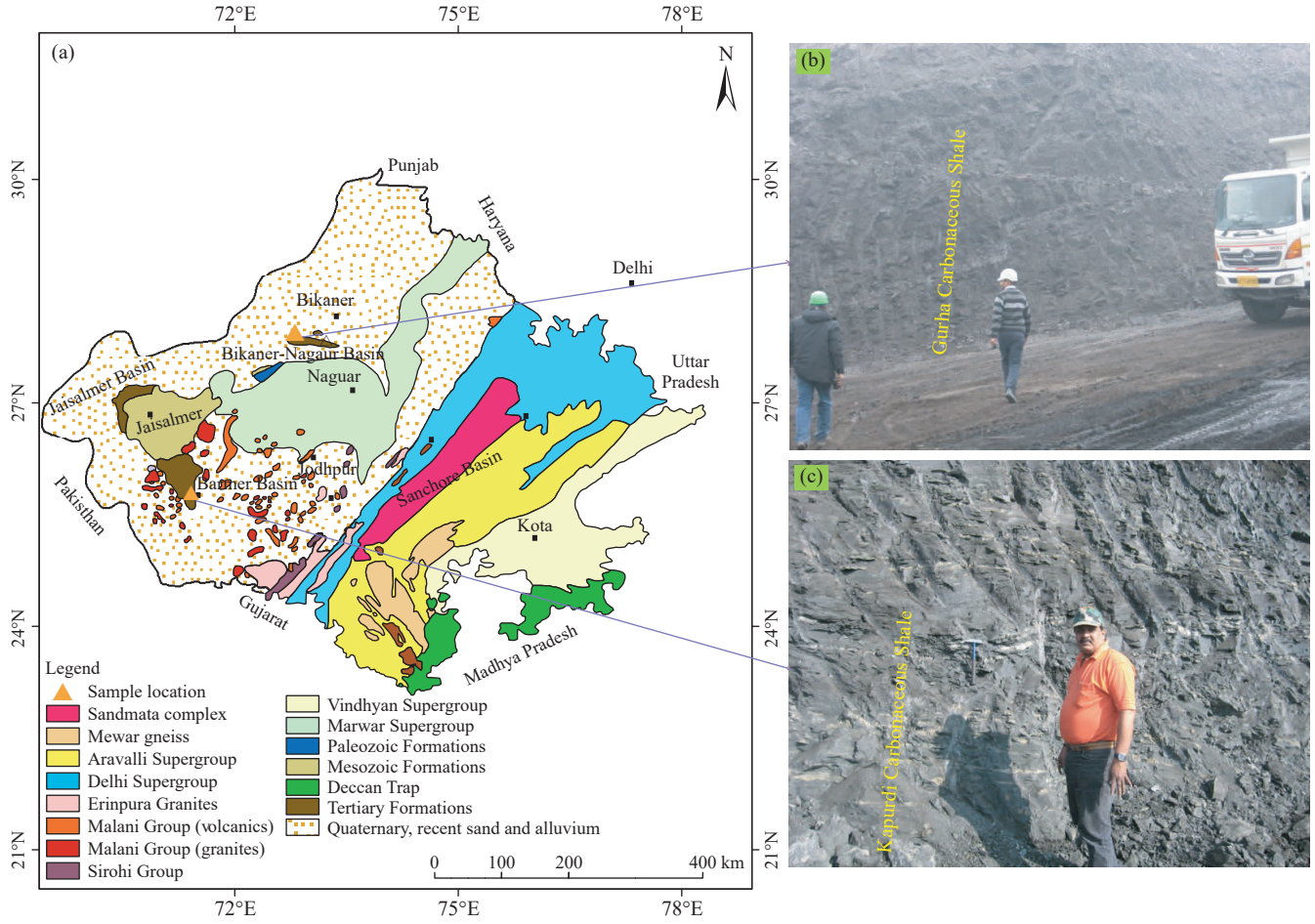

Fig. 1. a–Geological map of Rajasthan showing Bikaner-Nagaur and Barmer Basin (after Kumar A et al., 2022) with shale sampling location; sampling outcrop from b–Gurha mine and c–Kapurdi mines.

rocks for hydrocarbon generation (Kar NR et al., 2022). Lignite and carbonaceous shale deposits of Rajasthan mainly occur in Gurha, Barsinghsar, Matasukh, Giral, Kapurdi, and Sonari areas of the Bikaner-Nagaur and Barmer basins (Kumar A et al., 2020; Singh AK et al., 2020; Kumar A et al., 2022). Additionally, these deposits are mainly found in the Paleogene–Eocene Palana and Akli formations (Kumar A et al., 2020; Singh AK et al., 2020; Kumar A et al., 2022).

The lignite deposits in these two basins have been extensively investigated by Singh PK et al. (2016a), Singh AK and Kumar A (2017a, 2017b), Singh AK and Kumar A (2018a, 2018b), Singh AK et al. (2018), Kumar A et al. (2020), Mathews RP et al. (2020a), Rajak PK et al. (2021), Kumar A (2022), and Singh VP et al. (2022) to characterize their source rocks and evaluate their hydrocarbon-generation potential using the advance petro-geochemical techniques. In addition, several researchers (Singh PK et al., 2016b, 2016c; Singh VK et al., 2019; Rajak PK et al., 2019; Mathews RP et al., 2020b; Rajak PK et al., 2020; Chetia R et al., 2022; Kumar A et al., 2023; Kumar A et al., 2024) also extensively investigated the paleodepositional conditions in these two basins. Most studies have suggested that these lignite deposits contain mainly gas-prone (Type-III) and mixed hydrocarbon prone (Type II-III) kerogens, which are thermally immature organic matter (OM) and with good potential for gas generation. Furthermore, the reactive maceral (vitrinite and liptinite) contents in some lignite seams in the Bikaner-Nagaur basin suggest that these lignites are appropriate for liquefaction (Singh AK and Kumar A, 2017b). Notably, the associated carbonaceous shale partings have received limited research attention (Kumar A et al., 2022; Hakimi MH et al., 2023), regarding their source rock evaluation and hydrocarbon potential. The preliminary studies conducted in the basins have indicated that the Palaeocene and Eocene carbonaceous rocks are of economic interest because of their significant potential for exploitation in gas and oil generation. Therefore, the present research aims to strengthen our knowledge about source rock attributes of the organic-rich carbonaceous rocks associated with the lignite seams in the Bikaner-Nagaur and Barmer basins, which are of economic and scientific importance. The results of the present work can be useful for future exploration programs in western Rajasthan. Furthermore, the intensive exploration of the Paleocene-Eocene source rock system in the deeper structural units of the Barmer and Bikaner-Nagaur basins, where the Paleocene-Eocene carbonaceous shale deposits have reached maturity concerning oil generation, is paramount. An inclusive examination of the hydrocarbon potential and maturity of the Paleocene and Eocene carbonaceous shale deposits from the Kapurdi (Barmer Basin) and Gurha

(Bikaner-Nagaur Basin) area (Figs. 1a–c), Rajasthan, is conducted using geochemical and organic petrographic methods.

2. Geological setting

Rajasthan, which includes the Thar Desert in the northwest, is the largest state in India, accounting for 10.75% of the country's total land area (Roy AB and Jakhar SR, 2002). The basement of the region is characterized by various geological and tectonic events (Shukla A et al., 2023). The western region of Rajasthan has evolved through Cretaceous and Jurassic tectonic events. The detachment of the Indian plate from the Gondwana supercontinent during the Jurassic–Cretaceous era led to the formation of a rift basin in western Rajasthan and initiated the geological development of the region (Singh AK and Kumar A 2017a; Shukla A et al., 2023).

Due to the intracratonic sedimentation, three different sedimentary basins, the Bikaner-Nagaur, Barmer, and Jaisalmer basins developed across an area of approximately 120000 km^2 (Bhowmick PK, 2008). However, multiple phases of volcanic rock sequences and metasediment cycles occurred during the Precambrian in Rajasthan. These phases combined to form a banded gneiss structure that acts as the basement rock. These oldest basement gneiss rocks of the Archean age are collectively known as the Banded Gneissic Complex. The Proterozoic rocks are mostly restricted to the mountains and the peneplains of eastern Rajasthan comprise rocks of Malani, Aravalli, Delhi, and Vindhyan super groups (Fig. 1a).

The tectonic and lithological units in Rajasthan's Barmer and Bikaner-Nagaur basins range in age from the Archean to the Recent (Singh AK and Kumar A, 2020; Kumar A, et al. 2021; Fig. 1). The lithostratigraphic section of Rajasthan, ranging from the Barmer to the Bikaner-Nagaur Basins is presented in Fig. 2. These basins contain a mixture of carbonate, and clastic sediments of the Paleozoic (Cambrian-Permian) to the Cenozoic (Paleocene-Pliocene) era, as well as the Recent age (Fig. 2). The Cambrian Nagaur Formation is the deepest sedimentary succession in the Bikaner-Nagaur Basin (Fig. 2a), whereas the older stratigraphic sequences in the Barmer Basin comprise Lower–Middle Jurassic Formation (Fig. 2b).

In the Bikaner-Nagaur Basin, the basement rocks are composed of the Malani igneous suite of the Precambrian age. The Cambrian Nagaur Formation lies unconformably on the Precambrian basement rocks, which comprise siltstone, brick red clay stone, and sandstone with clay bands (Fig. 2a). The Nagaur Group, unconformably overlain by the Bap beds, consists of phyllite, gneiss, quartzite, pebbles and cobbles. Tertiary sediments are found in conformable contacts, such as the Jogira Formation (Fuller's earth, ferruginous marl), Marth Formation (ferruginous & gritty sandstone and siltstone), and Palana Formations (carbonaceous & black shale and lignite). The detailed lithological sequence of the Bikaner–Nagaur Basin is illustrated in Fig. 2a. The Barmer Basin consists of a rock sequence ranging from the Proterozoic to the recent era, partially covering Thar Desert's sands. The Lathi Formation of the Jurassic age sedimentary strata is unconformably found on top of the Precambrian age basement rocks (Malani igneous Suite). The Fatehgarh Formation comprises siliciclastics and bentonite beds and unconformably overlies the Lathi Formation. The Barmer Formation unconformably overlies the Fatehgarh. Above the Barmer Formation, the Akli Formation occurs with bentonite, sandstone, lignite, shale, and claystone. The Mandai Formation lies above the Akli sediments and consists of conglomerates and ferruginous

(a)

Age	Formation	Lithology
Recent & sub recent	---------	Blown sand
Eocene to Paleocene	Jogira Marth Palana	Fossiliferous marl, fullers earth, clayey marl Ferruginous sandstone, gritty sandstone, siltstone Carbonaceous and black shale, lignite, fullers earth
----------*Unconformity*----------		
Early Permian	Badhaura	Medium to coarse grained ferruginous sandstone, clays, shale and siltstone
----------*Unconformity*----------		
Early Carboniferous	Bap	Pebbles and cobbles, phyllite, slate, quartzite, gneiss, limestone
----------*Unconformity*----------		
Cambrian	Nagaur	Brick-red claystone, siltstone, sandstone with caly band
Precambrian	Malani Igneous suite	Malani rhyolites, tuffs, granites, porphyry, quartz veins and dykes

(b)

Age	Formation	Lithology
Recent	Recent deposits	Aeolian sand calcareous nodules
----------*Unconformity*----------		
Post Pliocene	Kapurdi	Fuller's Earth, variegated clay
Miocene-Pliocene	Mandai	Hard ferruginous sandstone
Eocene to Paleocene	Akli	Bentonite, sandstone, clay shale, and lignite
Cretaceous	Barmer	Sandstone, clay, siltstone
	Fatehgarh	Sandstone, bentonite, conglomerate, clay
----------*Unconformity*----------		
Lower-Middle Jurassic	Sornumill	Sandstone with fossil wood
	Lathi/Jaisalmer	Sandstone, limestone, conglomerate, marl
----------*Unconformity*----------		
Precambrian	Malani Rhyolite	Rhyolite, granite with dykes

Fig. 2. a–Generalized stratigraphic and lithological succession of Bikaner-Nagaur Basin and, b–Barmer Basin, Rajasthan (after Kumar A et al., 2020).

sandstone. The Kapurdi Formation overlies the Mandai Formation. Recent sediments of the Aeolian phases cover the older formations of the basin.

Fig. 2b depicts the detailed lithological succession of the Barmer Basin. The Paleocene-Eocene Palana Formation in the Bikaner-Nagaur Basin and the Akli Formation in the Barmer Basin, the primary subject of this investigation, are composed of mainly lignite and carbonaceous shales (Fig. 2). The Akli Formation in Barmer Basin is considered to have been deposited relatively close to the shoreline as demonstrated by palynological assemblages and microforaminiferal linings (Rajkumari P and Prasad GV, 2020). Rana RS et al. (2005) further suggested that the Akli Formation floodplain deposition occurs in subtropical to lagoons tropical with marine intrusions. The lignite-bearing Palana Formation in the Bikaner-Nagaur Basin includes land-derived spores-pollen assemblages, showing that the floristic linkage was tropical to subtropical and influenced by humid climatic conditions during peat accumulation (Mathews RP et al., 2020). The presence of flora assemblages in the Palana lignite and shale sediments is also suggests the presence of a mixed (rainforest/semi-arid/tropical evergreen) climatic condition in and around the mine area (Shukla A and Mehrotra RC, 2014, 2018).

3. Method of study

3.1. Sampling and sample preparation for analyses

Twelve carbonaceous shale samples were collected from the exposed mine face of Gurha (Fig. 1b) and Kapurdi (seven samples). The sampling method described by Schopf (1960) was followed during the sample collection from bottom to top. The collected samples were milled into ±18 mesh (approximate ⩽1 mm) and 72 mesh sizes using a mortar and pestle. The ±18 mesh particles were used for petrographic examination (i.e., macerals, mineral matter, and reflectance). For embedding the shale particulates mounts, epoxy resin, an epoxy hardener, a release agent, and sample cups were used. The shale pellets were ground for 3–5 min with a polishing machine using different silicon carbide waterproof papers (mesh size: 180, 320, 600, 800, 1000, 1200, and 2000; speed: 150–180 RPM) under continuous slow water flow. Buehler MicroCloth and MicroPolish gel (0.05 μm) were used to polish the pellets. The 72-mesh fraction of the samples was used for geochemical analyses.

3.2. Maceral analysis and reflectance measurement

Maceral composition analysis and reflectance measurement were performed using the Leica DM 2700P petrological microscope equipped with both reflected and UV–excitation light facilities, combined with a photometric system (MSP 200). The maceral identification was performed with mutually white incident and UV–excitation light. The petrographic analysis was based on the International Committee for Coal and Organic Petrology (ICCP) System 1994 (ICCP, 2001; Pickel W et al., 2017; Sýkorová I et al., 2005) and ISO norms (ISO 7404-3, 2009). The Petrog automatic point count stage system was used for quantitative maceral and mineral matter assessments, with a counting step of 0.4 mm was applied. Before conducting the reflectance measurement, the instrument was calibrated against reflectance standards with reflectance values of 0.420%, 0.902%, and 1.715%, respectively in immersion oil. Following the International Organization for Standardization (ISO) standard, approximately 100 random reflectance measurements of each polished block of ulminite maceral were taken (ISO 7404–5, 2009).

3.3. Geochemical analyses

Geochemical analyses were conducted on the carbonaceous shale samples, and their organic and inorganic matter compositions were measured. The elemental analysis was performed to determine the carbon, sulfur, hydrogen, nitrogen, and oxygen contents applying the American Society for Testing and Materials (ASTM) procedures ASTM D3176–15 (2002) and ASTM D5373–08 (2008). Rock-Eval pyrolysis facilities were obtained from the geochemical laboratories of Oil and Natural Gas Corporation (ONGC), India. The analysis was done using Pyrolyzer-6 instrument, following the procedure given by Espitalié J et al. (1977). In this device, a finely crushed (72 mesh) sample was heated in an inert atmosphere (nitrogen or helium) to a maximum temperature of 650°C. A detector (FID) was employed to sense the released hydrocarbons. The remaining carbons released were observed simultaneously using IR detectors. After the heat treatment, three chromatographic peaks (S_1, S_2, and S_3) were generated, and the TOC content and T_{max} values were determined. The S_1 peak is indicative of the volatized hydrocarbons in the rock at 350°C, the S_2 peak is assigned to the hydrocarbons generated from insoluble kerogen during heating from 350°C to 650°C, and the peak S_3 indicates the amount of CO_2 entrapped at 390°C during the thermal alteration of the oxygenated organic compounds.

4. Results

4.1. Petrography

The huminite, inertinite and liptinite macerals along with mineral matter (MM), were identified in the studied carbonaceous shale samples from Gurha and Kapurdi, as shown in Figs. 3 and 4. Accordingly, all the studied samples from Gurha and Kapurdi are dominated by mineral matter, mainly argillaceous minerals. The MM in the studied shale samples was dominated by clay as the groundmass, with carbonate, pyrite, and quartz (Figs. 3a–b, 4c, and 4e). Compared with the abundance of huminite macerals, hydrogen-rich liptinites display a high abundance in the Gurha shale (Fig. 3). In contrast, huminite derived from terrestrial organic matter dominates, with significant amount of liptinite detected in the Kapurdi shale (Fig. 4).

The huminite macerals display medium gray color, with a

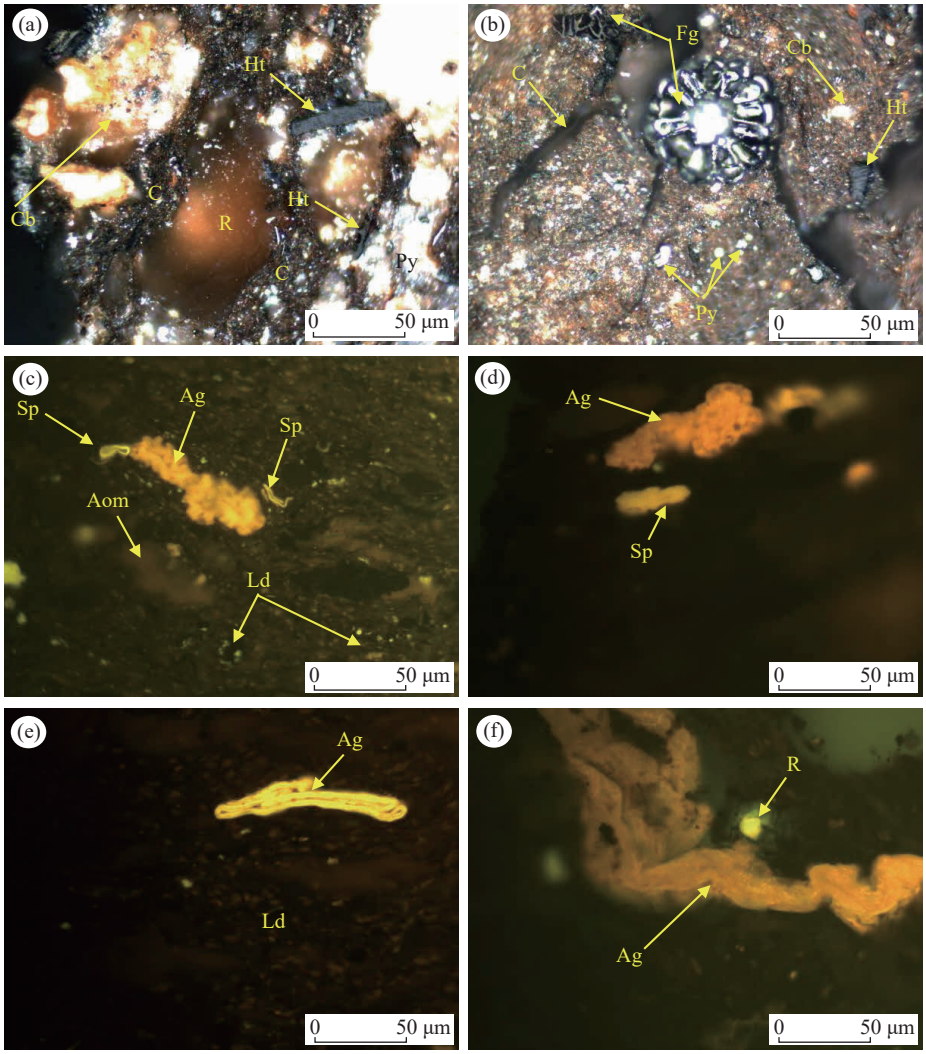

Fig. 3. Representative microphotographs of macerals and mineral matter observed in in Gurha shales from Bikaner-Nagaur Basin, Rajasthan. Ht/Bt–humodetrinite/solid bitumen; Cp–corpohuminite; Aom–amorphous organic matter; Ag–alginite; Sp–sporinite; R–resinite; Ld–liptodetrinite Fg–funginite; It-inertodetrinite Py–framboidal pyrite; C–clay; Cb–carbonate; Q–quartz.

reflectance value ($\%V_r$) <0.5% (Figs. 3a, b, and 4e). Most huminite macerals in studied samples appear as fine humic remains (<20 μm) associated with clay and carbonate minerals (Figs. 3a–b, and 4e). In addition, few rounded isolated patches of corpohuminite were observed in association with the mineral matter (Fig. 4e). The hydrogen-rich liptinite macerals in Gurha and Kapurdi include sporinite, resinite, liptodetrinite, alginite, and cutinite, which are presented as primary (structured) and secondary (unstructured) OM and display yellow to orange colour under UV light (Figs. 3c–f, 4a–b, 4d, and 4f).

In Gurha samples, most sporinites occur as thin walled isolated microspores (Figs. 3c–d), whereas in Kapurdi's shales, they occur as clusters of microspores (Fig. 4b) and microspores in ring form (Fig. 4d). Cutinite was also observed in the Kapurdi shale, which is characterized by an elongated threadlike structure with a serrated margin and dark orange fluorescence under UV light (Figs. 4e–f). These cutinite are derived from the cuticles of leaves. The alginite macerals were observed in both Gurha and Kapurdi and they were classified into telalginite and lamalginite based on their morphologies (Figs. 3d–f, and 4a). Lamalginite occurs as thick lamellae (Figs. 3d–f), whereas telalginite arises from algae and occurs as fan-shaped, flattened discs and discrete lenses (Fig. 4a).

Other unstructured macerals i.e., resinite and liptodetrinite also occur in the studied samples (Figs. 3e, 4d, and 4f). The resinite occurs in rounded, oval, and laminar shaped bodies (Figs. 4d and 4f). Liptodetrinite is a communal term for precursors of liptinite group macerals, identified as very fine detrital fragments (Figs. 3e and 4f). In the examined shales, inertodetrinites and funginites constitute the majority of the inertinite macerals, with few patches of semifusinite (Fig. 3b). In these shales, the funginites comprise fungal detritus as well as multicelled fungal bodies (Fig. 3b). In addition, the reflectance of the huminite maceral was measured. Based on the results, the mean values of the Gurha and Kapurdi samples are between 0.31% and 0.48% (Table 1). However, the reflectance of the huminite of the carbonaceous shales from the Kapurdi area is higher than that for the Gurha area, with mean value of 0.48% (Table 1).

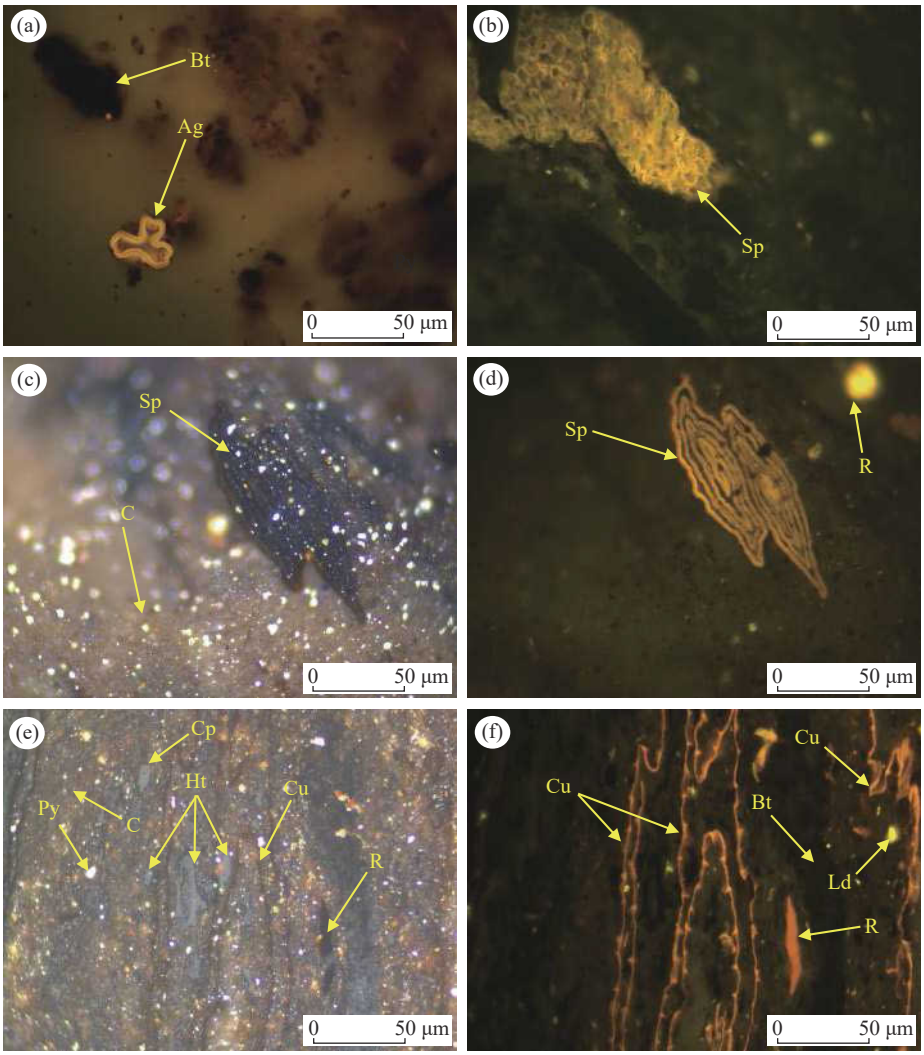

Fig. 4. Representative microphotographs of macerals and mineral matter observed in Kapurdi shales from Barmer Basin, Rajasthan. Ht/Bt–humodetrinite/solid bitumen; Ag–alginite; Sp–sporinite; Cu–cutinite; R–resinite; Ld–liptodetrinite Py–pyrite; C–clay.

Table 1. Ultimate elemental (CHNSO) analysis and vitrinite/huminite reflectance results of the Paleocene-Eocene carbonaceous shale samples from the Gurha and Kapurdi mines in the Bikaner-Nagaur and Barmer Basins of Rajasthan, western India.

Basin/Mine	Formation	Sample-ID	C	H	S	N	O	H/C	O/C	vitrinite/huminite reflectance (%)
			(in wt.%, daf)							
Bikaner-Nagaur/ Gurha	Palana	SGH-1	81.2	8.0	1.9	2.4	6.5	1.37	0.07	0.31
		SGH-2	67.1	6.4	1.8	2.3	22.4	1.33	0.29	0.33
		SGH-3	71.6	7.6	2.1	2.5	16.1	1.49	0.20	0.32
		SGH-4	78.2	8.4	1.9	2.5	9.0	1.50	0.10	0.37
		SGH-5	73.8	7.9	1.7	2.4	14.3	1.50	0.17	0.40
Barmer/ Kapurdi	Akli	SKP-1	59.6	5.1	1.2	1.9	32.3	1.03	0.41	0.35
		SKP-2	58.3	5.8	0.0	1.9	34.0	1.19	0.44	0.38
		SKP-3	63.1	5.4	0.9	1.8	28.7	1.03	0.34	0.41
		SKP-4	57.4	5.8	1.7	2.3	32.8	1.21	0.43	0.40
		SKP-5	46.9	5.0	1.7	1.9	44.5	1.28	0.71	0.44
		SKP-5	56.6	6.5	0.8	1.5	34.6	1.37	0.46	0.46
		SKP-7	57.1	7.3	0.0	2.3	33.3	1.53	0.44	0.48

4.2. Ultimate elemental results

The ultimate elemental (CHNSO) analysis provides information regarding the elemental configuration of fossil fuels. The ultimate elemental analysis and the quantitative analysis of the carbon and hydrogen elements are essential to comment on the utilization for evaluating the rank and the type of OM in the rocks.

Table 1 displays the CHNSO results for the examined shale samples, where it is shown that the carbon content in the

samples ranges from 46.9% to 81.2%, with an average value of 64.2%. The hydrogen content ranges from 5.0% to 8. 4%, whereas the nitrogen content ranges from 1.5% to 2.5%. The sulfur content was also measured and it ranges from 0.8% to 2.1% (Table 1). The oxygen content ranges from 6.5 to 44.5%. Notably, most of the studied samples from Gurha were rich in the carbon, hydrogen, and nitrogen (Table 1), whereas oxygen was relatively abundant in Kapurdi shales (Table 1). The H/C and O/C were also calculated based on the ultimate elemental analysis, the results show that the ratios in the studied samples range from 1.03 to 1.53 (mean 1.31) and 0.07 to 0.71 (mean 0.35), respectively (Table 1).

4.3. Geochemistry

The geochemical results of the studied Paleocene-Eocene carbonaceous shale samples, including the TOC content and several parameters are summarized in Table 2. The measured TOC contents of all the studied carbonaceous shales are high, ranging from 13.09 to 39.23% (Table 2). Most of the samples indicated a TOC content of > 20 wt% (21.75%–39.23%), whereas two samples exhibited a lower TOC content of 13.09%–15.48%, as shown in Table 2. The S_2 values yielded during the pyrolysis of kerogen are also high and generally consistent with TOC content (Fig. 5a). The S_2 values in the majority of the samples are greater than 30 mg HC/g rock (34.60–158.48 mg HC/g rock). However, the S_2 values of most of the studied samples from Gurha are higher than those of the Kapurdi (Table 2). T_{max} value is between 419°C and 429°C (Table 2).

Conversely, the pyrolysis data revealed that the S_1 yields in majority of the examined carbonaceous shale from Gurha is higher than those in the samples from Kapurdi (Table 2). The high S_1 has a positive correlation with TOC (R^2=0.69) (Fig. 5b). As revealed by the S_3 peak, the amount of CO_2 released during the pyrolysis of the oxygenated organic compounds was in the range of 2.64–14.80 mg CO_2/g rock (Table 2).

In addition, the HI, OI, PI values range from 208 to 516 mg HC/g rock, 15 to 46 mg CO_2/g rock, and 0.01 to 0.03 respectively (Table 2). Most of the studied carbonaceous shale from Gurha exhibited high HI values of >400 mg HC/g rock, up to 516 mg HC/g rock, whereas the studied shale samples from Kapurdi, exhibited relatively low HI values, varying from 208 to 375 mg HC/g rock (Table 2).

5. Discussion

5.1. OM abundance and the hydrocarbon generative potential

OM has the potential to generate diverse types of

Table 2. Geochemistry results of the Paleocene and Eocene carbonaceous shale samples from the Gurha and Kapurdi.

Basin/Mine	Formation	Sample-ID	S_1	S_2	S_3	T_{max} /°C	TOC/wt.%	HI	OI	S_2/S_3	PI	GP
Bikaner-Nagaur/ Gurha	Palana	SGH-1	1.26	112.27	3.18	429	21.75	516	15	35.36	0.01	113.53
		SGH-2	2.60	158.48	7.03	428	30.69	516	23	22.56	0.02	161.08
		SGH-3	2.04	121.22	8.26	425	29.75	407	28	14.67	0.02	123.26
		SGH-4	3.90	137.69	14.80	419	32.40	425	46	9.30	0.03	141.58
		SGH-5	2.96	137.38	11.05	423	29.41	467	38	12.44	0.02	140.34
Barmer/ Kapurdi	Akli	SKP-1	0.78	56.07	5.42	424	26.53	211	20	10.35	0.01	56.85
		SKP-2	0.84	51.77	8.04	426	24.75	209	32	6.44	0.02	52.61
		SKP-3	0.78	55.48	5.45	425	26.66	208	20	10.18	0.01	56.26
		SKP-4	0.41	35.76	6.58	422	15.48	231	42	5.44	0.01	36.17
		SKP-5	0.57	34.60	2.64	424	13.09	264	20	13.13	0.02	35.17
		SKP-5	1.89	76.23	8.74	425	22.10	345	40	8.27	0.02	78.12
		SKP-7	4.40	145.93	6.22	428	39.23	372	16	23.46	0.03	150.33

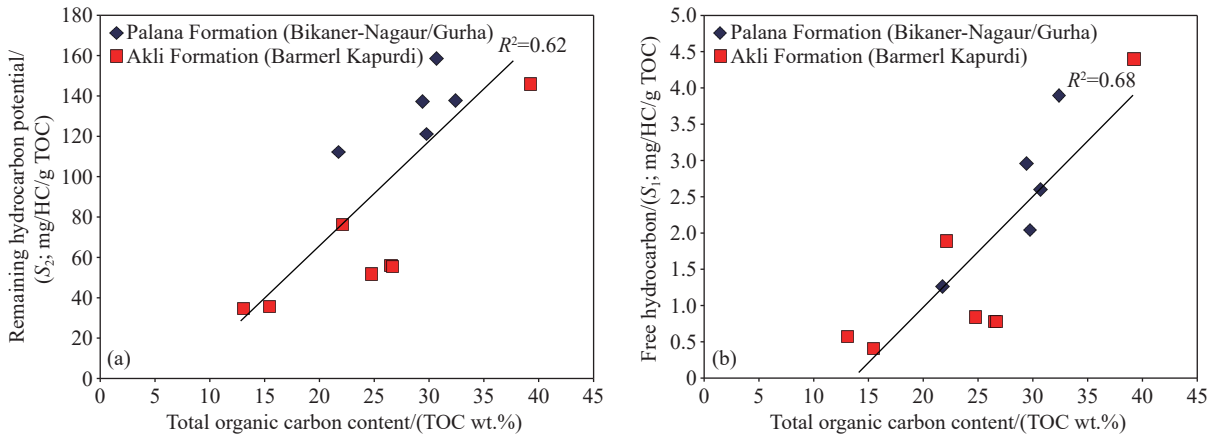

Fig. 5. Correlation of TOC with a–remaining hydrocarbon potential (S_2) and b–free hydrocarbon (S_1).

hydrocarbons; therefore, it is necessary to determine the abundance of OM in source rocks (Bordenave ML et al. 1993). To evaluate the hydrocarbon potential, the abundance of OM in a source rock is broadly used as a suitable indicator (Bordenave ML et al. 1993; Sun T et al., 2014). The TOC content in weight percentage indicates the OM richness as well as hydrocarbon generation potential (Peters KE, 1986; Peters KE et al., 1994). According to Katz BJ and Lin F (2014), a TOC content of >1% in a source rock suggests a favorable petroleum generation potential.

In the current research, the measured TOC contents of all the shale samples from the Gurha and Kapurdi are provided in Table 2, where it is shown that the studied samples have high TOC contents in the range of 13.09-39.23 wt%. Most of the studied samples have TOC contents of more than 4%, indicating that the Paleocene and Eocene shales in the Bikaner-Nagaur and Barmer basins are brilliant source rocks for hydrocarbon generation. The TOC contents were further combined with petroleum yields (GP=S_1+S_2). A minimum GP of 30 mg HC/g rock is required for a source rock to generate a good amount of hydrocarbon (Peters KE, 1986; Bordenave ML et al., 1993). According to the programmed pyrolysis results, the GP values of the studied shale samples is more than 30 mg HC/g rock and up to 161.08 mg HC/g rock (Table 2), highlighting their strong capability to generate hydrocarbons. Based on geochemistry results, we infer that the studied Paleocene and Eocene shales in the Bikaner-Nagaur and Barmer basins primarily have excellent generative potential (Fig. 6).

5.2. Kerogen characteristics and their implication on the petroleum generative potential

The kerogen characteristics and petroleum generative potential of the studied Paleocene and Eocene carbonaceous shales in the Barmer and Bikaner-Nagaur basins were assessed based on the results of the programmed pyrolysis and ultimate elemental analyses, along with the maceral analysis. The HI and OI parameters are employed to recognize the bulk kerogen types (Bordenave ML et al., 1993; Peters KE et al., 1994; Hakimi MH et al., 2013). The organic matter can be categorized under Type-I (>600 mg HC/g TOC), Type–II (600–300 mg HC/g TOC), Type–II–III (300–200 mg HC/g TOC), and type–III (200–50 mg HC/g TOC) (Hunt JM, 1995; Mastalerz M et al., 2018; Goodarzi F et al., 1990).

Here, the studied Paleocene-Eocene carbonaceous shales under consideration comprise dominantly Types II and II/III kerogen, with HI values ranging from 203 to 516 mg HC/g TOC (Table 2). However, the studied samples from the Gurha area exhibit high HI values of more than 400 mg HC/g TOC, whereas other samples from the Kapurdi area exhibit relatively low HI values between 208 and 372 mg HC/g TOC (Table 2). We observed that the examined carbonaceous shale samples from the Gurha area comprise dominantly Type II kerogen as showed by OI vs. HI diagram (Fig. 7a). The high contributions of the hydrogen-rich Types II and II/III kerogen are well corroborated with the T_{max} vs. HI cross plot results (Fig. 7b). The existence of these types of kerogens is also consistent with the high H/C atomic ratio derived from the

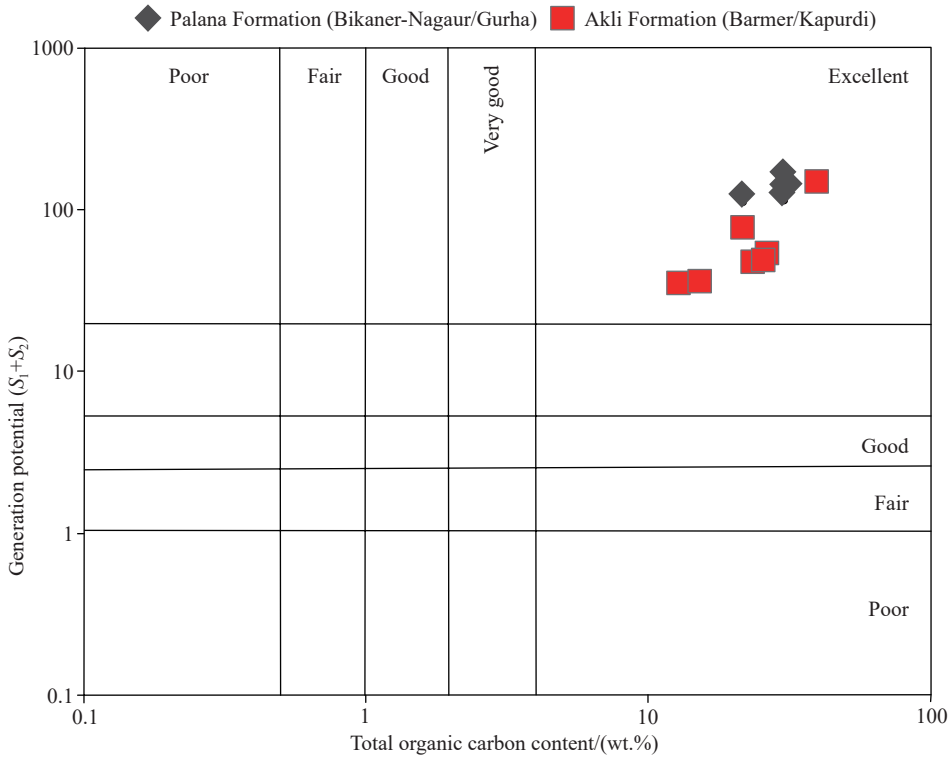

Fig. 6. Relationship between total organic carbon (TOC) content with petroleum generation (GP; S_1+S_2) of Rajasthan lignite (Peters KE et al., 1994).

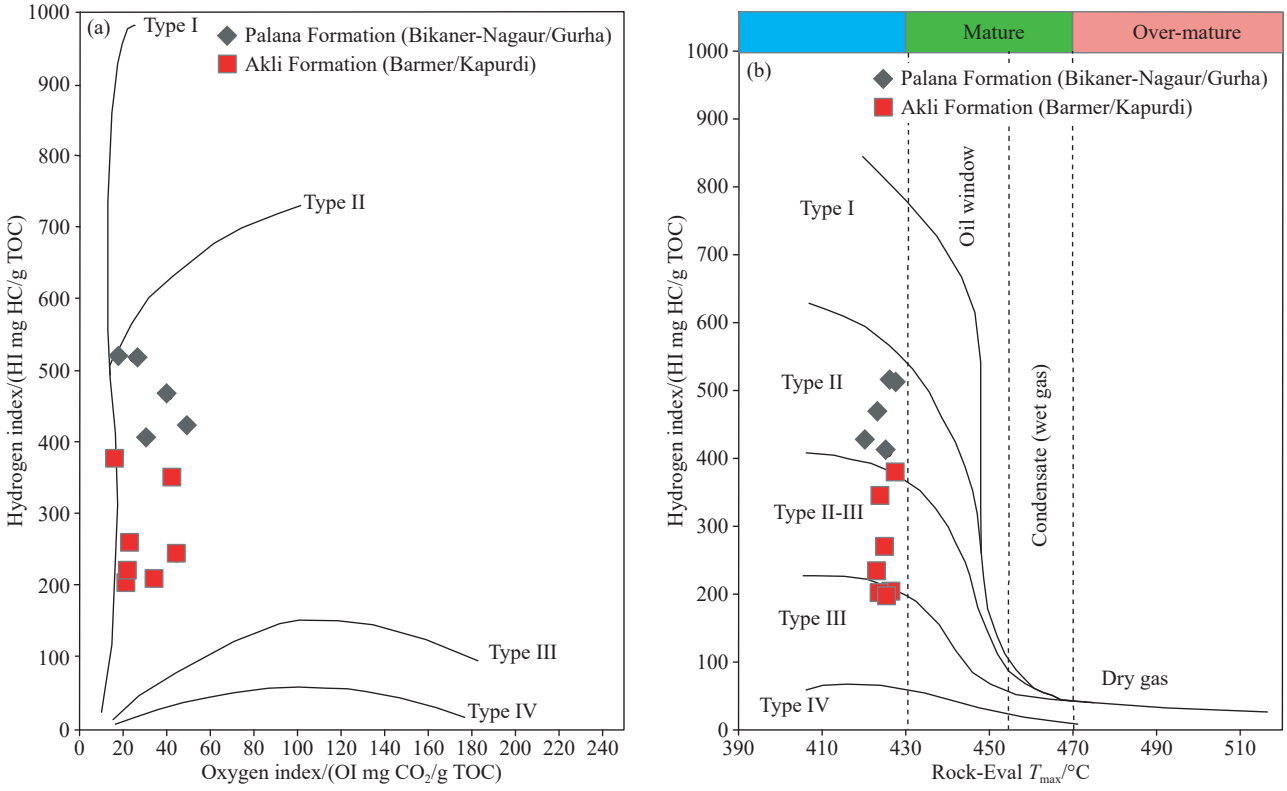

Fig. 7. Classification of kerogen type and assessment of the maturity based on Rock Eval-pyrolysis plots A–hydrogen index (HI) versus oxygen index (OI) (afterPeters KE, 1986); B–HI versus T_{max} (afterMukhopadhyay PK et al., 1995).

CHNSO analysis results (Table 1). The studied samples have high H/C atomic ratios of more than 1, indicating hydrogen-rich kerogen types (Tissot P and Welte DH, 1984). The interpretation of the hydrogen-rich kerogen in the studied carbonaceous shales is corroborated by the H/C and O/C plot, which specifies the presence of hydrogen-rich, with mainly Types II kerogen (Fig. 8).

Apart from the kerogen type, the analysis indicates that these carbonaceous shales are currently expected to release both oil and gas, with a high oil generative potential exhibited by the carbonaceous shale samples in the Gurha area. The same can also be concluded from the cross plots of TOC vs. HI and S_2/S_3 (Fig. 9). However, the variation in the organic matter (kerogen type) and generation potential of the Paleocene–Eocene carbonaceous shales is probably attributed to the different sources of the organic matter input. In this regard, we refer to the maceral composition obtained by petrography, revealing that the examined samples contain elevated levels of huminite and liptinite, alongside lesser amounts of inertinite macerals (Figs. 3 and 4). The dominance of liptinite and huminite over inertinite in the studied samples indicates the presence of hydrogen-rich Type II and II/III kerogens. This indicates that they can generate both oil and gas, although they have a high oil generation potential as evidenced by the high amounts of liptinite macerals. The presence of the liptinite –rich, oil-prone Type II kerogen (Fig. 3) is corroborated by the high HI values (> 400 mg HC/ g TOC) in the majority of the studied samples from the Gurha area in the Bikaner-Nagaur Basin (Figs. 7 and 8) and the H/C atomic ratio of more than 1.3 (Fig. 8). However, the relatively low current HI characteristics (208–372 mg HC/g TOC and H/C<1.2) in the samples from the Kapurdi area are consistent with the high contributions of huminite with amount of liptinite macerals (Fig. 4), indicating the dominance of mixed Type II and III kerogens (Figs. 8–10).

5.3. Thermal Maturity of OM

The thermal alteration of the organic source rocks with time, relative to the hydrocarbon generation potential is termed the thermal maturity of the source rock (Peters KE et al., 1994). Organic matter maturity is achieved when temperature and time-driven physicochemical changes convert organic-rich source rocks to oil, or/and wet gas, followed by dry gas and pyrobitumen (Peters KE et al., 1994). A thermally immature source rock can produce only microbial gases because the organic matter has undergone diagenesis without a distinct temperature effect (Mastalerz M et al., 2018). Thermally mature organic matter under the oil window can generate oil, having temperatures ranging from 60°C to 159°C, whereas thermally post-mature organic matter in the gas window zone, having temperatures ranging from 150°C to 200°C, can generate gaseous hydrocarbons (Mastalerz M et al., 2018).

The organic matter maturity is one of the critical parameters applied in oil and gas exploration programs to assess the thermal antiquity of sedimentary basins (Mastalerz M et al., 2018; Zheng G et al., 2003; Katz BJ and Lin F,

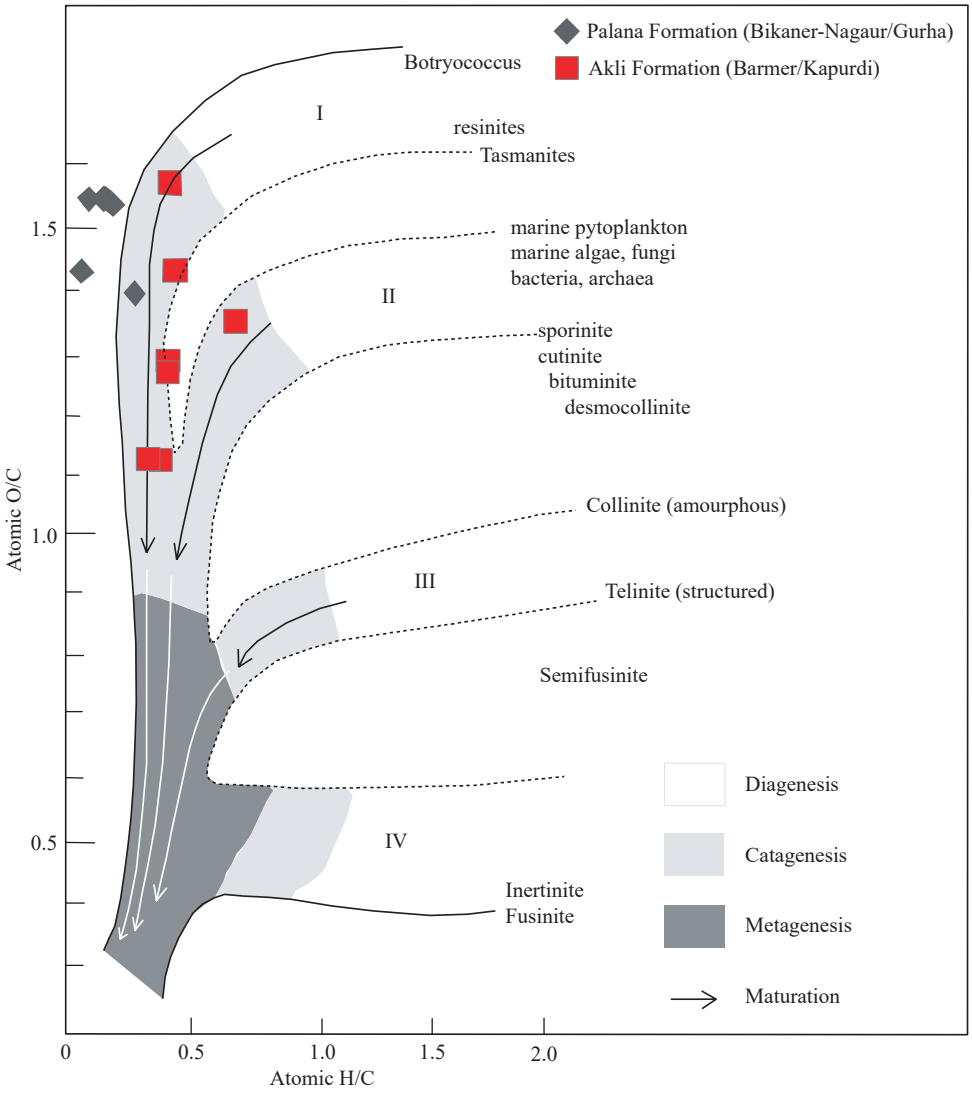

Fig. 8. Relationship between atomic ratios H/C and O/C for the shale samples of Bikaner-Nagaur and Barmer Basin, Rajasthan.

2021). The petrographic study (reflectance), coupled with Rock–Eval parameters, is used to interpret the rank and maturity of a source rock (Hakimi MH et al., 2013; Katz BJ and Lin F, 2021). Several thermal maturation indicators were principally used to assess the maturity level of the analysed shale samples, including the vitrinite reflectance and T_{max} and PI data. The vitrinite/huminite reflectance is a significant primary guide for source rock assessments (Espitalié J, 1986; Katz BJ and Lin F, 2021). The vitrinite reflectance increases uniformly with heating over geological time (coalification). Therefore, the vitrinite reflectance is a reliable parameter for estimating thermal maturity and for recognizing the effective paleotemperature. This parameter also provides insightful information regarding the maturity of OM and the evolution of the petroleum production (Mukhopadhyay PK, 1994).

In this study, the vitrinite/huminite reflectance measurements range between 0.31% and 0.48%, implying that the studied Paleocene-Eocene carbonaceous shales from the Barmer and Bikaner-Nagaur basins are thermally immature and cannot yet generate commercial amounts of oil. However, the maturity of the studied shale samples was also assessed using of the T_{max} and PI pyrolysis data. The T_{max}, derived from the pyrolysis graph, is one of the most widely used indicators of OM's thermal maturity (Espitalié J et al., 1977; Tissot P and Welte DH, 1979; Peters KE, 1986; Espitalié J, 1986; Katz BJ and Lin F, 2021; Hazra B et al., 2022).

The thermal maturity of the Gurha and Kapurdi shale has also been evaluated by based on the T_{max} and PI (Peters KE, 1986; Tissot P and Welte DH, 1984; Mukhopadhyay PK et al., 1995). Following the guidelines of Peters KE (1986), PI and T_{max} values lower than 0.1 and 435°C, respectively, indicate organic matter immaturity. The T_{max} and PI values in the studied samples from Gurha and Kapurdi range from 419°C to 429°C (<435°C; Table 2) and 0.01–0.03 (<0.1; Table 2), respectively, indicating immaturity of the OM. This contention is further supported by the good correlation between T_{max} and PI and the huminite reflectance (Fig. 10). The plot of HI *vs.* T_{max} also suggests the immaturity of the OM concerning the generation of hydrocarbon (Fig. 7b).

Although this investigation has provided valuable perceptions into the hydrocarbon generation potential of the

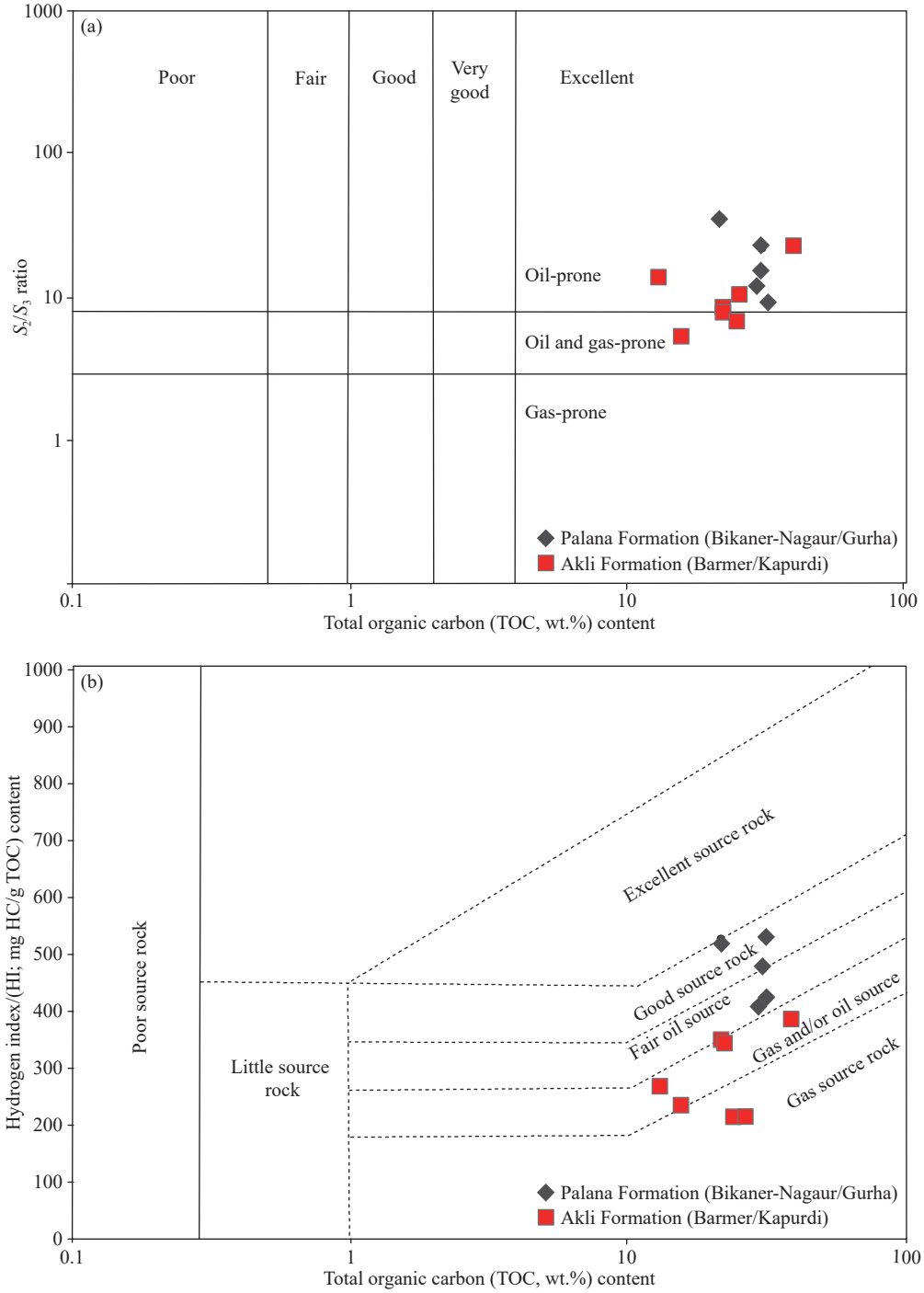

Fig. 9. Relationship between a–TOC content and S_2/S_3 yield; b–TOC content and HI (Peters KE et al., 1994).

Paleocene-Eocene carbonaceous rocks in the Barmer and Bikaner-Nagaur Basins, it is vital to acknowledge certain limitations. First, the possibility of our research was limited to definite geological formations in western Rajasthan, and therefore, the extrapolation of findings to other regions should be done with carefulness. Moreover, the study relied on specific analytical techniques and methodologies, such as organic petrography and, Rock-Eval pyrolysis which, while widely accepted, have their inherent limitations. The data obtained from these approaches deliver a snapshot of the hydrocarbon potential, and further studies employing a broader range of techniques could offer a more comprehensive understanding. Furthermore, the temporal and spatial variability within the study area may introduce uncertainties in the generalization of our results. Recognizing these limitations is vital for interpreting the findings and apprising future research instructions.

6. Conclusions

The following significant inferences were drawn concerning the nature and composition of OM, source rock properties, and thermal maturity, and their implications on the

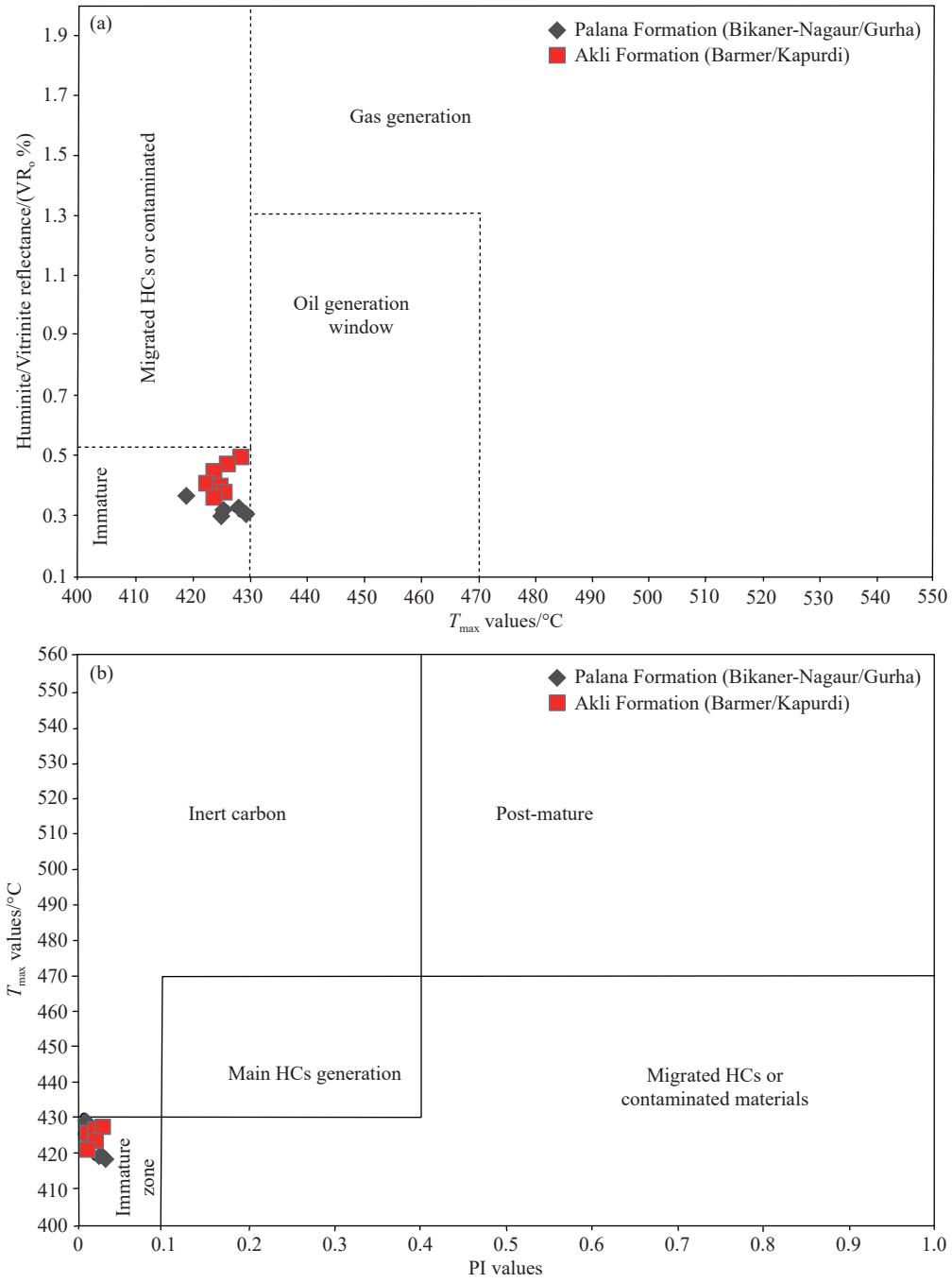

Fig. 10. Main stage of evolution (maturation) of the organic matter in the analyzed samples from Bikaner-Nagaur and Barmer Basin, showing maturity level, the plot of T_{max} with a–huminite reflectance, b–production index.

hydrocarbon generation potential of the shale deposits.

(i) The carbonaceous shale samples from the Gurha and Kapurdi mines are excellent source rocks for hydrocarbon generation based on their high organic matter content, with TOC contents ranging of >10% to 39.23%.

(ii) Different geochemical characteristics together with microscopic investigation reveals that the studied carbonaceous shales contain mainly hydrogen-rich Types II and II/III kerogens; thus, they can generate oil and gas, but exhibit high oil generation potentials.

(iii) According to the kerogen microscopy results, all the studied samples from the Paleocene-Eocene formations are dominated by mineral matter, with significant amounts of maceral. The carbonaceous shales from the Bikaner-Nagaur Basin are dominated by oil-prone liptinite over the huminite and inertinite macerals, whereas the huminite and liptinite macerals are dominant in the carbonaceous shale samples from the Barmer Basin.

(iv) Numerous maturity indicators and their corresponding low values reveal that the studied Paleocene-Eocene carbonaceous shale samples from the Gurha and Kapurdi mines are thermally immature and cannot yet generate in commercial amounts.

(v) The above characteristics can serve as a foundation for

future unconventional and conventional oil exploration in the deeper structural units of the Barmer and Bikaner-Nagaur Basins, where the Paleocene and Eocene formations have reached the main oil generation window and could release commercial amounts of oil.

CRediT authorship contribution statement

Alok Kumar conducted the laboratory analysis and prepare the first draft of manuscript. Khairul Azlan Mustapha, Alok K. Singh, and Mohammed Hail Hakimi supervised the research and reviewed the manuscript before submission. Ali Y. Kahale, Waqas Naseem and Hijaz Kamal Hasnan provided English editing and made modifications to the figures in the manuscript. All authors discussed the results and contributed to the final manuscript.

Declaration of competing interest

The authors declare no conflicts of interest.

Acknowledgment

The University of Malaya's postdoctoral fellowship program has been acknowledged by the first author and is associated with grant number IF064-2019. The authors also thank to Director RGIPT for allowing them to conduct this research and provide the facilities. We would like to express our gratitude to the Department of Science and Technology (Project No. SB/S4/ES-681/2013), Government of India, for their support. The authors extend their sincere appreciation to the Researchers Supporting Project number (RSPD2024R546) at King Saud University in Riyadh, Saudi Arabia.

References

ASTM D3176-15 2002. Standard Practice for Ultimate Analysis of Coal and Coke. In Annual Book of ASTM Standards. American Society for Testing and Materials West Conshohocken, PA, 1–3.

ASTM D5373 2008. Standard Test Methods for Instrumental Determination of Carbon, Hydrogen, and Nitrogen in Laboratory Samples of Coal, 1–11.

Bhowmick PK. 2008. Phanerozoic petroliferous basins of India. Glimpses of Geoscience research in India, 253–268.

Bordenave ML, Espitalié J, Leplat PO, Oudin JL, Vandenbroucke M. 1993. Screening techniques for source rock evaluation. Applied Petroleum Geochemistry, 217–278.

Chetia R, Mathews RP, Singh PK, Sharma A. 2022. Conifer-mixed tropical rainforest in the Indian Paleogene: New evidences from terpenoid signatures. Palaeogeography, Palaeoclimatology, Palaeoecology, 596, 110980. doi:10.1016/j.palaeo.2022.110980

Espitalié J, Laporte JL, Madec M, Marquis F, Leplat P, Paulet J, Boutefeu A. 1977. Rapid Method for Characterizing the Source Rocks, Their Petroleum Potential and Their Degree of Evolution. Revue de l'Institut Francais du Petrole, 32, 23–42. doi: 10.2516/ogst:1977002.

Espitalié J. 1986. Use of Tmax as a maturation index for different types of organic matter. Comparison with vitrinite reflectance. In: Burrus, J. (Ed.), Thermal Modelling in Sedimentary Basins. Editions Technip, Paris, 475–496.

Goodarzi F, Gentzis T, Yiakkoupis P. 1990. Petrographic characteristics and depositional environment of Greek lignites I: Drama Basin, northern Greece. Journal of Coal Quality, 9(1), 26–37.

Hakimi MH, Abdullah WH, Sia SG, Makeen YM. 2013. Organic geochemical and petrographic characteristics of Tertiary coals in the northwest Sarawak, Malaysia: implications for palaeoenvironmental conditions and hydrocarbon generation potential. Marine and Petroleum Geology, 48, 31–46. doi: 10.1016/j.marpetgeo.2013.07.009.

Hakimi MH, Kumar A, Singh AK, Lashin A, Rahim A, Varfolomeev MA, Yelwa NA, Mustapha KA. 2022. Geochemistry and organic petrology of the bituminite shales from the Kapurdi mine, Rajasthan of NW India: implications for waxy oil generation potential. Journal of Petroleum Exploration and Production Technology, 1–17. doi:10.1007/s13202-022-01597-9

Hazra B, Katz BJ, Singh DP, Singh PK. 2022. Impact of siderite on Rock-Eval S3 and oxygen index. Marine and Petroleum Geology, 143, 105804. doi: 10.1016/j.marpetgeo.2022.105804.

Hunt JM. 1995. Petroleum geochemistry and geology (textbook). Petroleum Geochemistry and Geology (Textbook). (2 nd Ed.), WH Freeman Company.

International Committee for Coal Petrology (ICCP) 2001. The new inertinite classification (ICCP System 1994). Fuel, 80, 459–471. doi:10.1016/S0016-2361(00)00102-2

ISO 7404-2. 2009. Methods for the Petrographic Analysis of Bituminous Coal and Anthracite–Part 2: Method of preparing coal samples. International Organization for Standardization, ISO, Geneva.

Kar NR, Mani D, Mukherjee S, Dasgupta S, Puniya MK, Kaushik AK, Biswas M, Babu EVSSK. 2022. Source rock properties and kerogen decomposition kinetics of Eocene shales from petroliferous Barmer basin, western Rajasthan, India. Journal of Natural Gas Science and Engineering, 100, 104497. doi: 10.1016/j.jngse.2022.104497.

Katz BJ, Lin F. 2014. Lacustrine basin unconventional resource plays: Key differences. Marine and Petroleum Geology, 56, 255–265. doi: 10.1016/j.marpetgeo.2014.02.013.

Katz BJ, Lin F. 2021. Consideration of the limitations of thermal maturity with respect to vitrinite reflectance, Tmax, and other proxies. AAPG Bulletin, 105(4), 695–720. doi: 10.1306/09242019261.

Kumar A, Singh AK, Paul D, Kumar A. 2020. Evaluation of hydrocarbon potential with insight into climate and environment present during deposition of the Sonari lignite, Barmer Basin Rajasthan. Energy and Climate Change, 1, 100006. doi: 10.1016/j.egycc.2020.100006.

Kumar A. 2022. Tertiary Coal and Lignite Deposits of India and their Source Rock Potential: A Review on the Contribution of the Indian Coal Petrologists. Journal of the Geological Society of India, 98(12), 1745–1753. doi: 10.1007/s12594-022-2246-0.

Kumar A, Singh AK, Paul D, Kumar A. 2021. Paleoenvironmental, paleovegetational, and paleoclimatic changes during Paleogene lignite formation in Rajasthan, India. Arabian Journal of Geosciences, 14, 2350. doi: 10.1007/s12517-021-08638-3.

Kumar A, Hakimi MH, Singh AK, Abdullah WH, Zainal Abidin NS, Rahim A, Mustapha KA, Yelwa NA. 2022. Geochemical and Petrological Characterization of the Early Eocene Carbonaceous Shales: Implications for Oil and Gas Exploration in the Barmer Basin, Northwest India. ACS omega, 7(47), 42960–42974. doi: 10.1021/acsomega.2c05148.

Kumar OP, Gopinathan P, Naik AS, Subramani T, Singh PK, Sharma A, Maity S, Saha S. 2023. Characterization of lignite deposits of Barmer Basin, Rajasthan: insights from mineralogical and elemental analysis. Environmental Geochemistry and Health, 45, 6471–6493. doi: 10.1007/s10653-023-01649-x.

Kumar OP, Naik AS, Gopinathan P, Subramani T, Singh V, Singh PK, Shukla UK, Prabhu A. 2024. Petrographic and geochemical analysis of Barmer Basin Paleogene lignite deposits: Insights into depositional environment and paleo-climate. Journal of Geochemical Exploration, 256, 107335. doi: 10.1016/j.gexplo.2023.107335.

Mastalerz M, Drobniak A, Stankiewicz AB. 2018. Origin, properties, and implications of solid bitumen in source-rock reservoirs: A review. International Journal of Coal Geology, 195, 14–36. doi: 10.1016/j.coal.2018.05.013.

Mathews RP, Singh BD, Singh VP, Singh A, Singh H, Shivanna M, Dutta S, Mendhe VA, Chetia R. 2020a. Organo-petrographic and geochemical characteristics of Gurha lignite deposits, Rajasthan, India: Insights into the palaeovegetation, palaeoenvironment and hydrocarbon source rock potential. Geoscience Frontiers, 11(3), 965–988. doi: 10.1016/j.gsf.2019.10.002.

Mathews RP, Chetia R, Agrawal S, Singh BD, Singh PK, Singh VP, Singh A. 2020b. Early Palaeogene climate variability based on n-alkane and stable carbon isotopic composition evidenced from the Barsingsar lignite-bearing sequence of Rajasthan. Journal of the Geological Society of India, 95, 255–262. doi: 10.1007/s12594-020-1423-2.

Mukherjee M, Misra S. 2018. A review of experimental research on Enhanced Coal Bed Methane (ECBM) recovery via CO_2 sequestration. Earth-Science Reviews, 179, 392–410. doi: 10.1016/j.earscirev.2018.02.018.

Mukhopadhyay PK. 1994. Vitrinite reflectance as maturity parameter: petrographic and molecular characterization and its applications to basin modeling. ACS Publications, ACS Symposium Series, 570, 1–24. doi:10.1021/bk-1994-0570.ch001

Mukhopadhyay PK, Wade JA, Kruge MA. 1995. Organic facies and maturation of Jurassic/Cretaceous rocks, and possible oil-source rock correlation based on pyrolysis of asphaltenes, Scotian Basin, Canada. Organic Geochemistry, 22(1), 85–104. doi: 10.1016/0146-6380(95)90010-1.

Peters KE. 1986. Guidelines for evaluating petroleum source rock using programmed pyrolysis. AAPG bulletin, 70(3), 318–329. doi: 10.1306/94885688-1704-11D7-8645000102C1865D.

Peters KE, Cassa MR, Magoon LB, Dow WG. 1994. The petroleum system—From source to trap. American Association of Petroleum Geologists Memoir, 60, 93–120. doi: 10.1306/M60585.

Pickel W, Kus J, Flores D, Kalaitzidis S, Christanis K, Cardott BJ, Misz-Kennan M, Rodrigues S, Hentschel A, Hamor-Vido M, Wagner N. 2017. Classification of liptinite–ICCP System 1994. International Journal of Coal Geology, 169, 40–61. doi: 10.1016/j.coal.2016.11.004.

Rajkumari P, Prasad GV. 2020. New chondrichthyan fauna from the Palaeogene deposits of Barmer district, Rajasthan, western India: Age, palaeoenvironment and intercontinental affinities. Geobios, 58, 55–72. doi: 10.1016/j.geobios.2019.11.002.

Rajak PK, Singh VK, Singh PK, Singh MP, Singh AK. 2019. Environment of paleomire of lignite seams of Bikaner-Nagaur basin, Rajasthan (W. India): petrological implications. International Journal of Oil, Gas and Coal Technology, 22(2), 218–245. doi:10.1504/IJOGCT.2019.102782

Rajak PK, Singh VK, Singh AL, Kumar N, Kumar OP, Singh V, Kumar A, Rai A, Rai S, Naik AS, Singh PK. 2020. Study of minerals and selected environmentally sensitive elements in Kapurdi lignites of Barmer Basin, Rajasthan, western India: implications to environment. Geosciences Journal, 24, 441–458. doi: 10.1007/s12303-019-0029-4.

Rajak PK, Singh VK, Kumar A, Singh V, Rai A, Rai S, Singh KN, Sharma M, Naik AS, Mathur N, Singh PK. 2021. Study of Hydrocarbon Source Potential of Kapurdi Lignites of Barmer Basin, Rajasthan, Western India. Journal of the Geological Society of India, 97, 836–842. doi: 10.1007/s12594-021-1782-3.

Rana RS, Kumar K, Loyal RS, Sahni A, Rose KD, Mussell J, Singh H, Kulshreshtha SK. 2006. Selachians from the Early Eocene Kapurdi Formation (Fuller's Earth), Barmer District, Rajasthan. Journal of the Geological Society of India, 67(4), 509–522.

Roy AB, Jakhar SR. 2002. Geology of Rajasthan (Northwest India) precambrian to recent. Scientific Publishers.

Schopf JM. 1960. Field description and sampling of coal beds (p. 67). Washington, DC: US Government Printing Office.

Shukla A, Mehrotra RC. 2014. Paleoequatorial rain forest of western India during the EECO: evidence from Uvaria L. fossil and its geological distribution pattern. Historical Biology, 26(6), 693–698. doi: 10.1080/08912963.2013.837903.

Shukla A, Mehrotra RC. 2018. Early Eocene plant megafossil assemblage of western India: Paleoclimatic and paleobiogeographic implications. Review of palaeobotany and palynology, 258, 123–132. doi: 10.1016/j.revpalbo.2018.07.006.

Singh AK, Kumar A. 2017a. Petro-chemical characterization and depositional paleoenvironment of lignite deposits of Nagaur, Western Rajasthan, India. Environmental Earth Sciences, 76, 692. doi: 10.1007/s12665-017-7004-z.

Singh AK, Kumar A. 2017b. Liquefaction behavior of Eocene lignites of Nagaur Basin, Rajasthan, India: A petrochemical approach. Energy Sources, Part A: Recovery, Utilization, and Environmental Effects, 39(15), 1686–1693. doi:10.1080/15567036.2017.1370514

Singh AK, Kumar A. 2018a. Organic geochemical characteristics of Nagaur lignites, Rajasthan, India, and their implication on thermal maturity and paleoenvironment. Energy Sources, Part A: Recovery, Utilization, and Environmental Effects, 40(15), 1842–1851. doi:10.1080/15567036.2018.1487480

Singh AK, Kumar A. 2018b. Petrographic and geochemical study of Gurha Lignites, Bikaner Basin, Rajasthan, India: Implications for thermal maturity, hydrocarbon generation potential and paleodepositional environment. Journal of the Geological Society of India, 92, 27–35. doi: 10.1007/s12594-018-0949-z.

Singh AK, Kumar A. 2020. Assessment of thermal maturity, source rock potential and paleodepositional environment of the Paleogene lignites in Barsingsar, Bikaner–Nagaur Basin, Western Rajasthan, India. Natural Resources Research, 29, 1283–1305. doi: 10.1007/s11053-019-09502-8.

Singh PK, Rajak PK, Singh VK, Singh MP, Naik AS, Raju SV. 2016a. Studies on thermal maturity and hydrocarbon potential of lignites of Bikaner–Nagaur basin, Rajasthan. Energy Exploration & Exploitation, 34(1), 140–157. doi: 10.1177/0144598715623679.

Singh PK, Rajak PK, Singh MP, Singh VK, Naik AS. 2016b. Geochemistry of kasnau-matasukh lignites, Nagaur basin, Rajasthan (India). International Journal of Coal Science & Technology, 3, 104–122. doi: 10.1007/s40789-016-0135-0.

Singh PK, Rajak PK, Singh MP, Singh VK, Naik AS, Singh AK. 2016c.

Peat swamps at Giral lignite field of Barmer basin, Rajasthan, Western India: understanding the evolution through petrological modelling. International Journal of Coal Science & Technology, 3, 148–164. doi: 10.1007/s40789-016-0137-y.

Singh AK, Kumar A, Hakimi MH. 2018. Organic geochemical and petrographical characteristics of the Nagaur lignites, Western Rajasthan, India and their relevance to liquid hydrocarbon generation. Arabian Journal of Geosciences, 11, 1–15. doi: 10.1007/s12517-018-3744-7.

Singh VK, Rajak PK, Singh PK. 2019. Revisiting the paleomires of western India: An insight into the early Paleogene lignite Corridor. Journal of Asian Earth Sciences, 171, 363–375. doi: 10.1016/j.jseaes.2018.08.031.

Singh VP, Singh BD, Mathews RP, Singh A, Mendhe VA, Mishra S, Banerjee M. 2022. Paleodepositional and Hydrocarbon Source-Rock Characteristics of the Sonari Succession (Paleocene), Barmer Basin, NW India: Implications from Petrography and Geochemistry. Natural Resources Research, 31(5), 2943–2971. doi: 10.1007/s11053-022-10079-y.

Shukla A, Jasper A, Uhl D, Mathews RP, Singh VP, Chandra K, Chetia R, Shukla S, Mehrotra RC. 2023. Paleo-wildfire signatures revealing co-occurrence of angiosperm-gymnosperm in the early Paleogene: Evidences from woody charcoal and biomarker analysis from the Gurha lignite mine, Rajasthan, India. International Journal of Coal Geology, 265, 104164. doi: 10.1016/j.coal.2022.104164.

Sun T, Wang C, Duan Y, Li Y, Hu B. 2014. The organic geochemistry of the Eocene–Oligocene black shales from the Lunpola Basin, central Tibet. Journal of Asian Earth Sciences, 79, 468–476. doi: 10.1016/j.jseaes.2013.09.034.

Sýkorová I, Pickel W, Christanis K, Wolf M, Taylor GH, Flores D. 2005. Classification of huminite—ICCP System 1994. International Journal of Coal Geology, 62(1-2), 85–106. doi: 10.1016/j.coal.2004.06.006.

Tissot P, Welte DH. 1984. Petroleum formation and occurrence. Springer-verlag.

Zheng G, Duan Y, Takano B, Luo B, Cheng K, Zhang Y. 2003. Pyrolysis studies on the conversion of vitrinite reflectance and the primary productivity of various non-marine source rocks in China. Journal of Asian Earth Sciences, 22(4), 353–361. doi: 10.1016/S1367-9120(03)00061-0.